



# *In-situ* remediation of acid mine drainage from abandoned coal mine by filed pilot-scale passive treatment system: Performance and response of microbial communities to low pH and elevated Fe

Haiyan Chen<sup>a,c</sup>, Tangfu Xiao<sup>b,\*</sup>, Zengping Ning<sup>a</sup>, Qian Li<sup>b</sup>, Enzong Xiao<sup>b</sup>, Yizhang Liu<sup>a</sup>, Qingxiang Xiao<sup>a,d</sup>, Xiaolong Lan<sup>a,e</sup>, Liang Ma<sup>a,c</sup>, Fanghai Lu<sup>f</sup>

<sup>a</sup> State Key Laboratory of Environmental Geochemistry, Institute of Geochemistry, Chinese Academy of Sciences, Guiyang 550081, China

<sup>b</sup> Key Laboratory for Water Quality and Conservation of the Pearl River Delta, Ministry of Education, School of Environmental Science and Engineering, Guangzhou University, Guangzhou 510006, China

<sup>c</sup> University of Chinese Academy of Sciences, Beijing 100049, China

<sup>d</sup> School of Tourism Management, Guizhou University of Commerce, Guiyang 550014, China

<sup>e</sup> School of Chemistry and Environmental Engineering, Hanshan Normal University, Chaozhou 521041, China

<sup>f</sup> School of Materials and Metallurgical Engineering, Guizhou Institute of Technology, Guiyang 550003, China

## ARTICLE INFO

### Keywords:

Acid mine drainage (AMD)  
*In-situ* bioremediation  
Microbial community  
Iron

## ABSTRACT

A field pilot-scale passive treatment system was developed for *in-situ* bioremediation of acid mine drainage (AMD). The microbial community and its variation were analyzed. The data proved that 93.7% of total soluble Fe and 99% of soluble Fe(II) could be removed by the system. Principal coordinates analysis (PCoA) showed that a low pH and an elevated Fe concentration within the system created a unique microbial community that was dominated by acidophilic iron-oxidizing bacteria and iron-reducing bacteria. Canonical correlation analysis (CCA) indicated that the pH, iron content and total sulfur jointly determined the composition of the microbial communities. Species of *Ferrovum*, *Delftia*, *Acinetobacter*, *Metallibacterium*, *Acidibacter* and *Acidiphilium* were highly enriched, which promoted the removal of iron. Furthermore, the results revealed important data for the biogeochemical coupling of microbial communities and environmental parameters. These findings are beneficial for further application of *in-situ* field bioreactors to remediate AMD.

## 1. Introduction

Acid mine drainage (AMD) is a global environmental issue encountered by sulfide-rich mining industries. As soon as fresh ore is exposed to oxygen, water and microorganisms, AMD is produced (Johnson and Hallberg, 2003; Simate and Ndlovu, 2014). Characterized by a low pH and high concentrations of heavy metals (e.g., Fe, Mn, Pb, Cr, Hg, Cd and As) and sulfate, AMD poses serious risks to surrounding surfaces and groundwater, as well as soil (Favas et al., 2016). Subsequently, life is threatened. It has been reported that in AMD-contaminated areas, heavy metals are potentially transferable to human beings, causing illness and death (Pruvot et al., 2006). Detailed effects of heavy metals and low pH on human health, plant life and aquatic life were reviewed by Simate and Ndlovu (2014).

To clean up AMD, two approaches have been used, namely active and passive treatments (Johnson and Hallberg, 2005). Active treatments include the application of alkaline chemicals or rocks to

neutralize acidity and precipitate metals (Johnson and Hallberg, 2005). However, these methods require continuous input, and for chemical/rock treatment, they also require the disposal of large volumes of secondary waste. By contrast, the passive treatment is considered a more promising approach since it relies on naturally biological, geochemical and physical processes to neutralize acidity and to oxidize or reduce and precipitate metals at low cost and with few maintenance requirements (Gazea et al., 1996; Akcil and Koldas, 2006). Passive treatment employs indigenous microorganisms from AMD to develop a bioreactor system and has been widely applied to remediate AMD at remote abandoned mine sites (Behum et al., 2011; Kalin and Caetano Chaves, 2003; Sun et al., 2016). Microorganisms are thought to play an important role in metal removal and acid reduction in bioreactor systems treating AMD (Kalin et al., 2006; Kalin and Caetano Chaves, 2003). Environmental variables are important factors that affect the microbial communities inhabiting passive AMD bioreactors. Recently, most studies of passive AMD bioreactor systems focused on the response of

\* Corresponding author.

E-mail address: [tfxiao@gzhu.edu.cn](mailto:tfxiao@gzhu.edu.cn) (T. Xiao).

<https://doi.org/10.1016/j.biortech.2020.123985>

Received 18 June 2020; Received in revised form 4 August 2020; Accepted 6 August 2020

Available online 08 August 2020

0960-8524/ © 2020 Elsevier Ltd. All rights reserved.

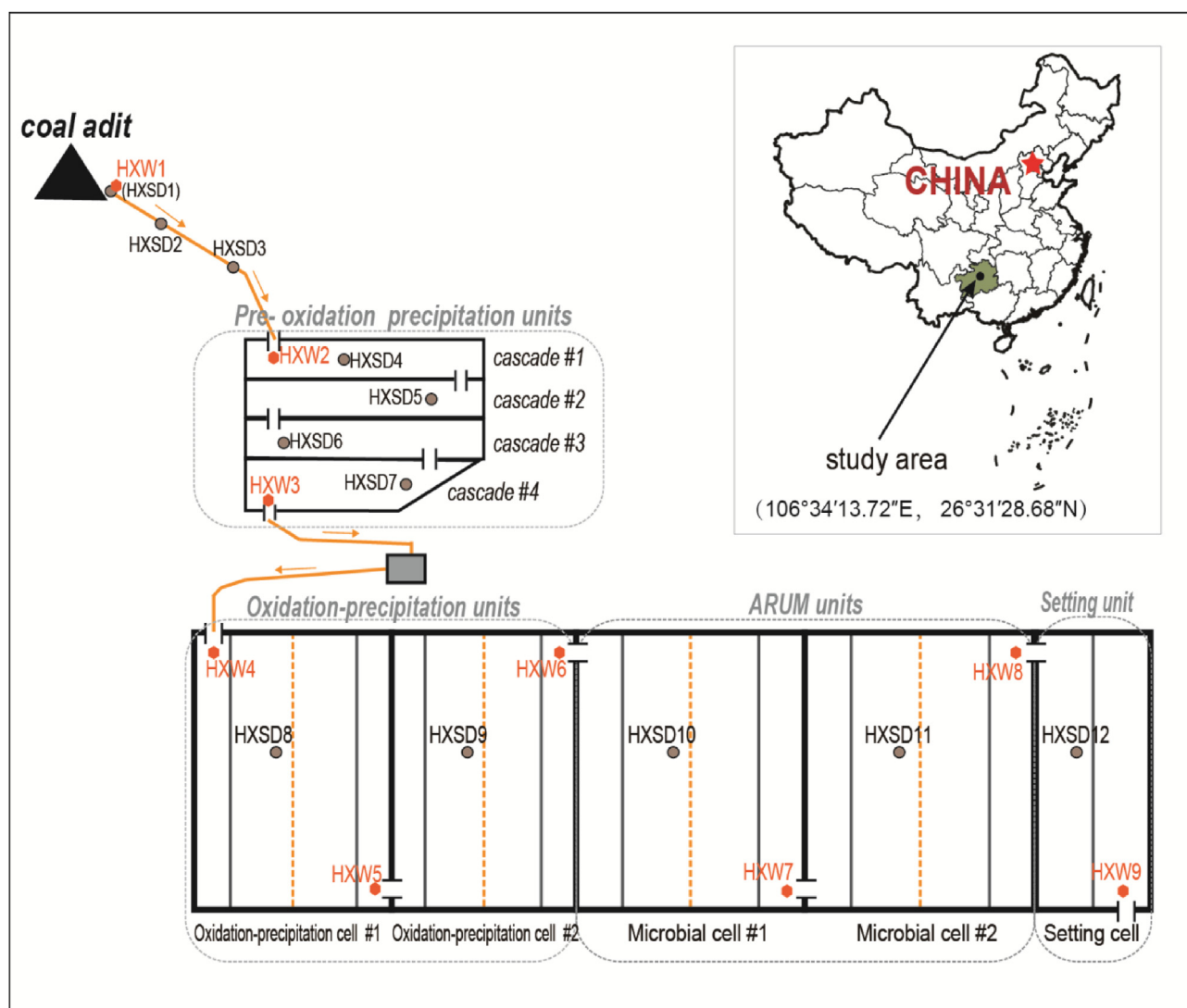


Fig. 1. Map showing pilot-scale passive treatment system components including water and sediment sampling sites (Nine AMD water sampling sites were named HXW1-HXW9; HXSD1-HXSD12 indicated sediment sample sites).

specific microorganisms to environmental factors during laboratory test (Bai et al., 2013; Vasquez et al., 2018; Zhou et al., 2018). However, it should be noted that the microbial communities are not universal for each remediation site, as the composition of AMD and environmental conditions differ at different sites. Thus, a pilot-scale study should be carried out to study the relation between environmental factors under field conditions and *in situ* microbial communities as well as their metabolic preference, which is crucial in maintaining, optimizing or developing an AMD bioreactor.

In the present study, following Kalin and Caetano Chaves, 2003, a field pilot-scale treatment system was constructed to passively treat AMD in an abandoned coal mine in Guizhou Province, Southwest China (Fig. 1). The AMD drains from the mine adit to downstream watercourses at a rate of 24.81 m<sup>3</sup>/d in the rainy season and 2.44 m<sup>3</sup>/d in the dry season. Since the coal seams were associated with pyritic geological strata, the AMD is extremely acidic (pH 2.70 ± 0.13) and contains a high concentration of Fe(II) (762.18 ± 136.52 mg/L) and SO<sub>4</sub><sup>2-</sup> (4133.67 ± 771.4 mg/L). Fe(II) is expected to be removed from the AMD by the passive treatment system, as it can react with dissolved oxygen to produce iron oxide precipitates. As of the writing of this paper, the pilot-scale passive treatment system has been running for > 6 years and has shown good performance in the removal of Fe(II). However, the system does not remove SO<sub>4</sub><sup>2-</sup> or neutralize acid very

well, although some amendments have been made. Thus, the objective of this study was to monitor the environmental parameters including concentrations of Fe(II) and Fe(total), pH, redox potential, electrical conductivity and temperature, as well as to characterize the indigenous microbial consortia in each unit of the treatment system. The results will help to figure out: 1) the relation between microbial consortia and environmental factors under an extremely low pH condition, 2) how Fe is removed and whether the microorganisms made contributions and 3) reason for the failure of acid neutralization. Our data also provide a reference for researchers who are planning to apply field-scale bioreactor systems to remediate AMD from similar mine sites.

## 2. Materials and methods

### 2.1. Treatment system description

A reinforced concrete treatment system was constructed in 2013 with a total volume of 682 m<sup>3</sup> and a residence time of 10 d during the wet season and 59 d during the dry season. The system consists of four units: a four-cell cascade aeration unit (Cascades #1–4 (approximately 3.5 m length × 5.0 m width × 0.3–0.4 m depth)), two oxidation-precipitation cells (oxidation-precipitation cell #1 (OC1, 8.5 m length × 11.0 m width × 1.9 m depth) and oxidation-precipitation cell

#2 (OC2, 8.5 m length  $\times$  11.0 m width  $\times$  1.7 m depth)), two microbial treatment cells (MC1 (10.5 m length  $\times$  11.0 m width  $\times$  1.5 m depth) and MC2 (10.5 m length  $\times$  11.0 m width  $\times$  1.3 m depth)) and one setting cell (4.0 length  $\times$  11.0 m width  $\times$  1.3 m depth) (Fig. 1). The AMD flows to the four units in sequence. The four-cell cascade aeration unit is designed to enhance the oxidation of Fe(II) by aeration and was implemented in 2014. The oxidation-precipitation cells are also used to oxidize and precipitate Fe(II). Three baffles and some PVC curtains were placed in each cell to assist in settling iron hydroxide particles. The two microbial treatment cells are designed to remove sulfate and the remaining Fe, and to neutralize acidity by alkalinity generating microorganisms such as sulfur-reducing bacteria (SRB) and iron-reducing bacteria (FeRB). With alkalinity generation, as the pH rises, the sulfide precipitates Fe(II) as iron sulfides. Consequently, the concentrations of both sulfate and Fe in the AMD are reduced. For this purpose, rice straw compost was added at the bottom of each microbial treatment cell to provide organic carbon and form microbial active sediment. Over compost, cattail (*Typha Linn.*) was planted in pots and configured as a mat by PVC tubing in June 2016. The living floating cattail cover can lower cell turbulence and oxygen dissolution, thereby enhancing the reducing conditions. The microbial treatment cell is also known as an acid reduction using microbiology (ARUM) cell.

Details on the AMD flow and treatment system can be found in Fig. 1. To treat the AMD, there are 4 stages in total. The AMD originates from the coal adit (HXW1) and falls to a slope terrain that has been stained by an orange or black iron crust. Along the slope, the effluent moves to the four-cell cascade aeration unit (pre-oxidation precipitation stage). Then, it flows to OC1 and OC2 in sequence (oxidation-precipitation stage). After being processed by microorganisms in microbial cells (MC1-MC2, ARUM stage), the effluent finally moves to the setting cell (setting stage). After all treatments, the effluent is discharged to a downstream creek.

## 2.2. Sampling and analysis

Due to poor transportation and a remote location, the AMD water samples were collected once a month in a twelve-month period from December 2016 to November 2017. The sampling sites were labeled as HXW1-HXW9 in orange in Fig. 1. These sites are the origin of the AMD (HXW1), the inlet and outlet of the four-cell cascade unit (HXW2 and HXW3) and the five (bio)remediation cells (HXW4-HXW9). A HACH HQ30d multimeter (HACH, Loveland, USA) was used to measure the pH, electronic conductivity (EC), Eh and temperature of the effluent at each site before sampling. The total Fe and Fe(II) in the water samples was measured using a spectrophotometric method (UV-9000s, METASH, Shanghai) with 1, 10-phenanthroline at 510 nm (Tamura et al., 1974). Anion including  $\text{SO}_4^{2-}$  was measured by ion chromatography (Dionex, ICS-90, Sunnyvale, CA, USA).

A total of 48 AMD sediment samples were collected from the coal adit (A), slope (B), pre-oxidation precipitation units (C), oxidation-precipitation units (D), ARUM units (E) and setting unit (F) in the treatment system from December 2016 to November 2017.

HXSD1-HXSD12 were used to label the sample sites in Fig. 1. In detail, a fresh sediment sample was collected from the outlet of the coal adit (HXSD1), two iron crust samples were collected from the slope terrain (upper 1–2 cm, HXSD2 to HXSD3), four sediment samples (iron crusts) from the four-cell cascade unit (HXSD4 to HXSD7) and five sediment samples from the rest five (bio)remediation cells (HXSD8 to HXSD12). The samples were taken once a season: 12 samples collected in December 2016 (winter, J1), 12 samples in March 2017 (spring, J2), 12 samples in July 2017 (summer, J3) and 12 samples in October 2017 (autumn, J4). Samples from the five (bio)remediation cells were collected with a PVC trap, and the samples from HXSD1 to HXSD7 were collected with a wide-mouth container. All samples were placed into sterile 50-ml tubes and kept in an ice box. Once back to the laboratory, parts of the samples were immediately stored at  $-80\text{ }^\circ\text{C}$  for further

microbial analysis. The rest were freeze-dried by a vacuum freeze-drying machine (FD-1–50), and then they were ground and sieved with a 200-mesh sieve for physical and chemical characterization as well as geochemical analysis.

To measure the pH and Eh of the sediment samples, 5 g of freeze-dried sediment powder was mixed with 10 mL of Milli-Q water and shaken for 30 min. After standing for a while, the pH was measured with an HACH HQ30d multi meter. To measure anions in the sediment samples, 2 g of freeze-dried sediment was mixed with 10 mL of Milli-Q water and shaken for 5 min, then left to equilibrate for 4 h. Afterward, the supernatant was centrifuged at  $3500 \times g$  for 15 min and filtered through a 0.45- $\mu\text{m}$  filter membrane, and then determined by using ion chromatography (Dionex, ICS-90, Sunnyvale, CA, USA). The total sulfur (TS), soluble sulfur, total hydrogen (TH) and total carbon (TC) in the sediments were measured using an elemental analyzer (Elementar, Hanau, Germany). The geochemical sequent extraction method (Poulton and Canfield, 2005) was applied to determine the Fe fractions in the sediments, i.e., carbonate-associated Fe ( $\text{Fe}_{\text{carb+AVS}}$ ), easily reducible oxides ( $\text{FeOX1}$ ) including ferrihydrite and lepidocrocite, crystalline oxide form ( $\text{FeOX2}$ ), and magnetite ( $\text{Fe}_{\text{mag}}$ ). The Fe content in each extractable fraction was measured using a spectrophotometric method (UV-9000 s, METASH, Shanghai) with 1, 10-phenanthroline at 510 nm (Tamura et al., 1974). The standard reference material GBW07310 (Chinese National Standard) was used for analytical quality control. Three measurements of a single sample were performed for each geochemical parameter.

## 2.3. DNA extraction, PCR and 16 rRNA gene sequencing and statistical analysis

Total genome DNA from samples was extracted using CTAB/SDS method. The DNA concentration and purity were monitored on 1% agarose gels. According to the concentration, the DNA was diluted to 1 ng/ $\mu\text{L}$  using sterile water. The 16S rRNA genes of distinct regions (V4) were amplified using the 515F/806R primer pairs with the barcode (Caporaso et al., 2012). All PCR reactions were carried out with Phusion® High-Fidelity PCR Master Mix (New England Biolabs). The library was sequenced on an Illumina HiSeq 2500 platform Novogene (Beijing, China), and 250 bp paired-end reads were generated.

Raw tags were generated by merging paired-end reads using FLASH (V1.2.7, <http://ccb.jhu.edu/software/FLASH/>) (Magoc and Salzberg, 2011) and quality filtered using QIIME v1.7.0 (Caporaso et al., 2010) to obtain high-quality clean tags. The tags were compared with the reference database (Gold database, [http://drive5.com/uchime/uchime\\_download.html](http://drive5.com/uchime/uchime_download.html)) using the UCHIME algorithm (UCHIME Algorithm, [http://www.drive5.com/usearch/manual/uchime\\_algo.html](http://www.drive5.com/usearch/manual/uchime_algo.html)) to detect chimeric sequences (Edgar et al., 2011), and then the chimeric sequences were removed (Haas et al., 2011). Finally, the Effective Tags were obtained. Sequences with  $\geq 97\%$  similarity were assigned to the same OTUs by Uparse software (Uparse v7.0.1001, <http://drive5.com/uparse/>) (Edgar, 2013). OTUs abundance information was normalized using a standard of sequence numbers corresponding to samples with the least number of sequences. Subsequent analysis was performed using this output-normalized data.

QIIME calculates both weighted and unweighted UniFrac, which are phylogenetic measures of beta diversity. Principal Coordinate Analysis (PCoA) was performed to obtain principal coordinates and visualize from complex, multidimensional data. A distance matrix of weighted or unweighted UniFrac among samples obtained previously was transformed to a new set of orthogonal axes, by which the maximum variation factor was demonstrated by the first principal coordinate, the second maximum by the second principal coordinate, and so on. PCoA analysis was displayed by the WGCNA package, stat packages and ggplot2 package in R software (Version 2.15.3). Unweighted Pair-Group Method with Arithmetic Means (UPGMA) Clustering was performed as a type of hierarchical clustering method to interpret the

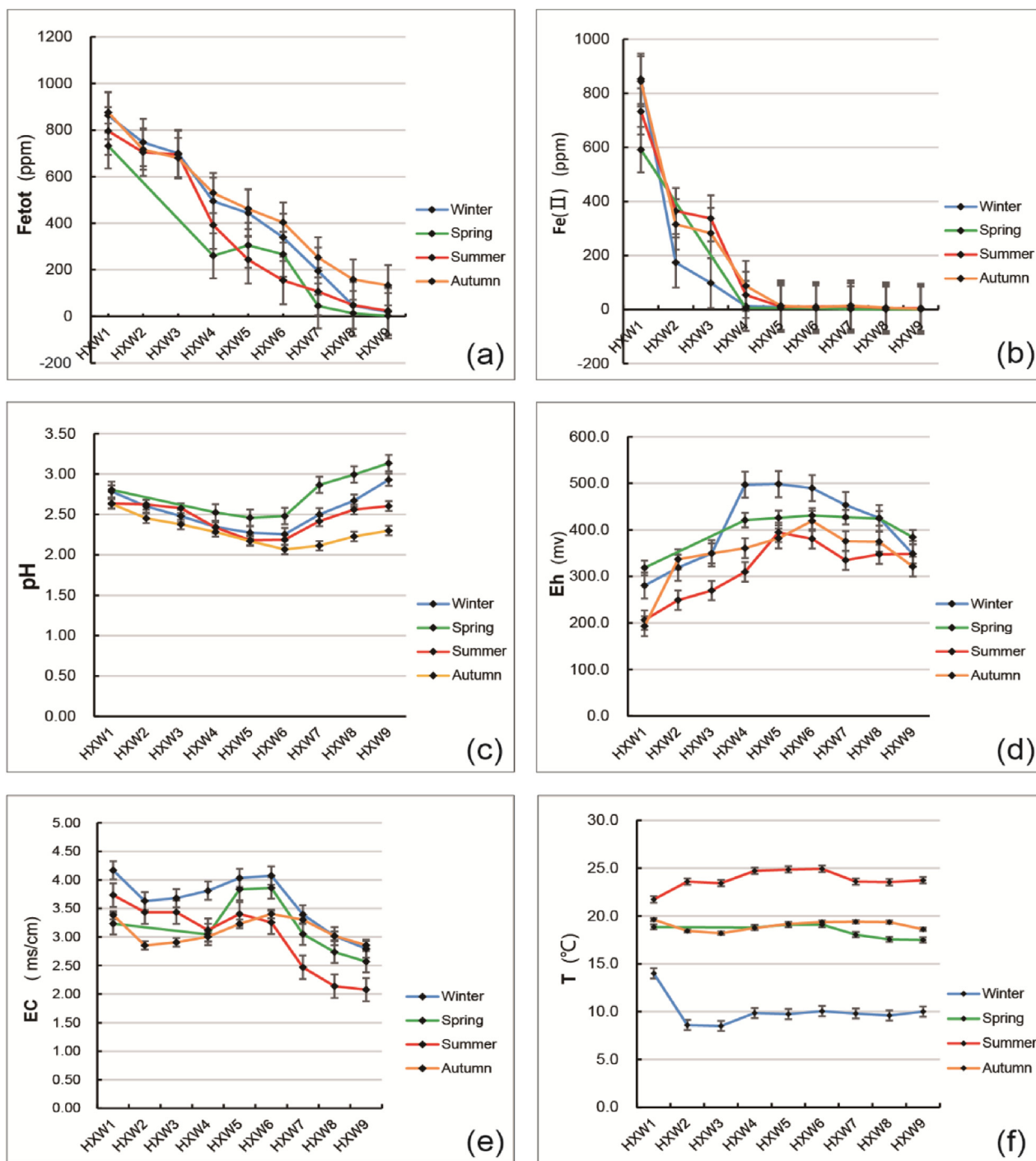


Fig. 2. Water physicochemical parameters from each monitoring point of treatment system. (a): Content of total Fe; (b): content of Fe(II); (c): pH; (d): Eh; (e): EC; (f): Temperature (T).

distance matrix using average linkage and was conducted by the QIIME software (Version 1.7.0). Canonical correspondence analysis (CCA) performed by the Novomagic platform (<https://magic.novogene.com/>) was used to identify the influence of geochemical parameters on microbial community structures.

### 3. Results and discussion

#### 3.1. Performance of in-situ pilot-scale passive treatment system

Environmental parameters were continuously monitored over the

course of one year, and the results can be found in Fig. 2. The downward curves in Fig. 2a illustrated that the detectable total Fe continued to decrease as the AMD passed through the system. After the overall treatment, 93.7% of the total soluble Fe was removed, as the concentration decreased from  $820.5 \pm 88.17$  mg/L (HXW1) to  $51.69 \pm 72.68$  mg/L (HXW9). According to Fig. 2b, Fe(II) oxidation mainly took place at the slope terrain and in the four-cell cascade aeration unit since the slope of the curves dramatically decreased from HXW4. Before the effluent entered OC #1, there was only  $45.94 \pm 47.59$  mg/L Fe(II), which means that 94% of Fe(II) had been oxidized. Finally,  $2.96 \pm 2.71$  mg/L Fe(II) was discharged. The results

**Table 1**Fe sequential extractable speciation in sediment samples (Mean of 4 season's  $\pm$  standard deviation).

Samples	Fe <sub>tot</sub> (mg/g)	Fe <sub>carb+AVS</sub> (mg/g)	FeOX1 (mg/g)	FeOX2 (mg/g)	Fe <sub>mag</sub> (mg/g)
HXSD1	414.73 $\pm$ 34.21	1.53 $\pm$ 0.44	257.61 $\pm$ 65.98	37.74 $\pm$ 9.08	3.88 $\pm$ 1.42
HXSD2	491.26 $\pm$ 16.39	0.92 $\pm$ 0.22	362.74 $\pm$ 17.2	27.97 $\pm$ 8.51	4.47 $\pm$ 1.37
HXSD3	477.29 $\pm$ 76.39	1.13 $\pm$ 0.53	379.51 $\pm$ 22.53	21.2 $\pm$ 3.7	3.11 $\pm$ 1.11
HXSD4	426.32 $\pm$ 20.13	1.36 $\pm$ 0.57	374.35 $\pm$ 39.2	21.41 $\pm$ 1.9	4.82 $\pm$ 2.72
HXSD5	451.25 $\pm$ 80.07	0.94 $\pm$ 0.37	368.97 $\pm$ 27.54	25.72 $\pm$ 4.85	5.43 $\pm$ 2.25
HXSD6	452.28 $\pm$ 33.36	0.5 $\pm$ 0.09	385.98 $\pm$ 24.71	27.83 $\pm$ 7.16	5.52 $\pm$ 0.87
HXSD7	441.81 $\pm$ 37.59	0.82 $\pm$ 0.31	358.2 $\pm$ 30.26	28.84 $\pm$ 2.73	5.37 $\pm$ 1.56
HXSD8	193.33 $\pm$ 66.81	0.84 $\pm$ 0.59	105.21 $\pm$ 27.54	21.51 $\pm$ 0.38	1.5 $\pm$ 0.09
HXSD9	213.76 $\pm$ 78.22	0.91 $\pm$ 0.78	122.22 $\pm$ 39.87	22.32 $\pm$ 1.54	1.46 $\pm$ 0.11
HXSD10	124.13 $\pm$ 20.44	0.07 $\pm$ 0.05	80.33 $\pm$ 22.15	10.38 $\pm$ 4.25	1.04 $\pm$ 0.2
HXSD11	127.37 $\pm$ 13.42	0.09 $\pm$ 0.06	87.46 $\pm$ 11.25	11.28 $\pm$ 2.3	0.93 $\pm$ 0.19
HXSD12	204.21 $\pm$ 18.55	0.55 $\pm$ 0.29	141.92 $\pm$ 20.89	18.85 $\pm$ 3.17	0.86 $\pm$ 0.54

also showed that the performance of the treatment system had certain seasonal differences, especially for Fe(II) removal (Fig. 2b), which was better in summer and autumn than in winter and spring. In the case of pH (Fig. 2c) it kept decreasing from  $2.7 \pm 0.14$  (HXW1) to  $2.22 \pm 0.17$  (HXW6) in the first two units, and kept increasing in the rest two units. At the outlet (HXW9) of the system, the pH was measured as  $2.68 \pm 0.29$ . The Eh increased continuously in the (pre)oxidation-precipitation cells. As the effluent entered the ARUM cells, the Eh started to decrease (Fig. 2d), indicating that the aquatic environments of the treatment system shifted from relatively oxidized to relatively reduced conditions. The EC was  $3.62 \pm 0.48$  mS/cm in the coal adit (Fig. 2e). It decreased along the treatment system and was finally measured as  $2.55 \pm 0.37$  mS/cm in the effluent. The decrease in EC along the system illustrated that the mineral content of the water was reduced. The results showed that the temperature of the AMD in the system fluctuated from 5 °C (winter) to 30 °C (summer) (Fig. 2f). In addition, the sulfate concentration also decreased from  $4133.67 \pm 771.40$  (HXW1) to  $2706.32 \pm 1130.52$  mg/L (HXW9) along the treatment system, with a removal rate of 34.52%.

All sediment samples contained a high content of Fe (Fe<sub>tot</sub>) (Table 1), ranging from  $414.73 \pm 34.21$  mg/g at the coal adit to  $204.21 \pm 18.55$  mg/g at the end of the treatment system. In the four Fe-extractable fractions, FeOX1, referring to amorphous and crystalline Fe (mainly ferrihydrite and lepidocrocite) (Oni et al., 2015), was predominant. The content of FeOX1 was high ( $> 100$  mg/g) in all samples but relatively low at HXSD10 ( $80.33 \pm 22.15$  mg/g). FeOX2 (crystalline Fe (oxyhydr)oxides, mainly goethite and hematite) (Oni et al., 2015) was predominant in HXSD1 ( $37.74 \pm 9.08$  mg/g), was relatively low in other samples and was lowest at HXSD10 ( $10.38 \pm 4.25$  mg/g). Comparatively, Fe<sub>carb+AVS</sub> and Fe<sub>mag</sub> accounted for relatively small portions of Fe<sub>tot</sub>. The sediments were also acidic, as the pH was  $< 3$  for all 48 samples. The total sulfur (TS) content observed along the system, decreased from  $1.21\% \pm 0.33\%$  to  $0.95\% \pm 0.06\%$ . All samples had a total carbon (TC) content of  $< 3\%$ , except for samples from the coal adit (HXSD1,  $5.45\% \pm 1.11\%$ ) and the MC2 (HXSD11,  $3.08\% \pm 1.43\%$ ).

From the above results, the treatment system in this study showed good performance in the removal of Fe under an extremely low pH condition, and three points should be emphasized. First, the aerobic process was necessary and important, since 99% of Fe(II) was oxidized and 65% of Fe was removed in the first two aerobic units (cascades #1-4 and OC #1-2) (Fig. 2). The removed Fe was precipitated, which was deduced from the results that a high content of Fe (a majority was in form of FeOX1 and FeOX2) was detected in the sediment (Table 1). Second, placing baffles and PVC curtains in OC #1-2 enhanced Fe removal, which was confirmed by the Fe<sub>tot</sub> in the effluent being  $715.75$  g/L and  $689.58$  g/L at the inlet and outlet of the four-cell cascade aeration unit, respectively, and only  $288.44$  g/L could be detected at the outlet of OC #2. Since iron hydroxide particles can form encrustments of various consistencies on all underwater surfaces, the baffle and curtains

increase the surface area to which the iron hydroxide particles can adsorb. Last, during the Fe removal process, microorganisms should play an important role. For Fe(II) removal, an important step is Fe(II) oxidation, and the chemical oxidation of Fe(II) occurs quite slowly at pH  $< 4$  (Johnson, 1998). The pH within our system was never higher than 2.7, which means that in the system biologically mediated Fe(II) oxidation occurred and promoted the oxidative precipitation of Fe(III) under low pH conditions. This is in accordance with other reports (Johnson & Hallberg, 2005; Larson et al., 2014).

### 3.2. Microbial composition and community structure in the treatment system

Microorganisms play an important part in effective remediation of AMD (Kalin et al., 2006; Kalin and Caetano Chaves, 2003). In this study, a total of 4,383,236 high quality sequencing reads were obtained from the 48 sediments, ranging from 80,000 to 99,968 reads per sample, and clustered into 4730 operational taxonomic units (OTUs). Forty-four phyla were identified, and *Proteobacteria* predominated in all samples with a mean relative abundance (MRA) of  $66.89 \pm 17.15\%$ . This phylum was more abundant in the coal adit than in the pilot-scale passive treatment system (Fig. 3a). *Actinobacteria* was the second most abundant phylum with MRA of  $7.57 \pm 4.54\%$ , followed by *Firmicutes* ( $5.3 \pm 8.14\%$ ) and *Acidobacteria* ( $4.87 \pm 4.95\%$ ). *Actinobacteria* and *Acidobacteria* were dominant in the ARUM units (MC1-MC2), and the abundance of *Firmicutes* in the ARUM units was the lowest compared with that in other AMD treatment units in the treatment system.

Genus level analysis can provide detailed information about the microorganisms. Thus, the bacterial genera across all samples were analyzed. Principal coordinate analysis (PCoA) at the OTU-level (97% sequence similarity) based on unweighted UniFrac indicated that distinct microbial communities developed in each unit of the treatment system (Fig. 4). Non-metric multidimensional scaling (NMDS) showed similar results. The MRAs of the dominant genera in the pre-oxidation precipitation units (cascades #1-4) were different from those in other units (Fig. 3b). More specifically, in the pre-oxidation precipitation units *Phyllobacterium*, *Delftia*, *Ferroplasma* and *Acinetobacter* were dominant, accounting for  $17.59 \pm 12\%$ ,  $13.03 \pm 10.6\%$ ,  $9.83 \pm 11.23\%$  and  $5.20 \pm 5.48\%$  of the MRA, respectively. In the oxidation-precipitation units (OC1-OC2), *Delftia* ( $9.53 \pm 10.03\%$ ), *Phyllobacterium* ( $8.29 \pm 9.03\%$ ) and *Metallibacterium* ( $8.23 \pm 7.02\%$ ) showed relatively higher abundances than those of other genera. *Acidiphilium* ( $9.88 \pm 6.95\%$ ), *Acidibacter* ( $8.43 \pm 4.19\%$ ) and *Metallibacterium* ( $7.33 \pm 4.68\%$ ) showed higher abundances than those of other genera in the two ARUM cells. The most abundant genera in the setting unit were *Acidiphilium* ( $14.66 \pm 8.57\%$ ), *Acidibacter* ( $8.48 \pm 3.79\%$ ), *unidentified\_Oxyphotobacteria* ( $6.87\% \pm 5.8\%$ ) and *Bacteroides* ( $5.48 \pm 9.56\%$ ) (Table 2).

A UPGMA tree based on the shared phylogenetic distance between each group indicated that distinct microbial communities developed

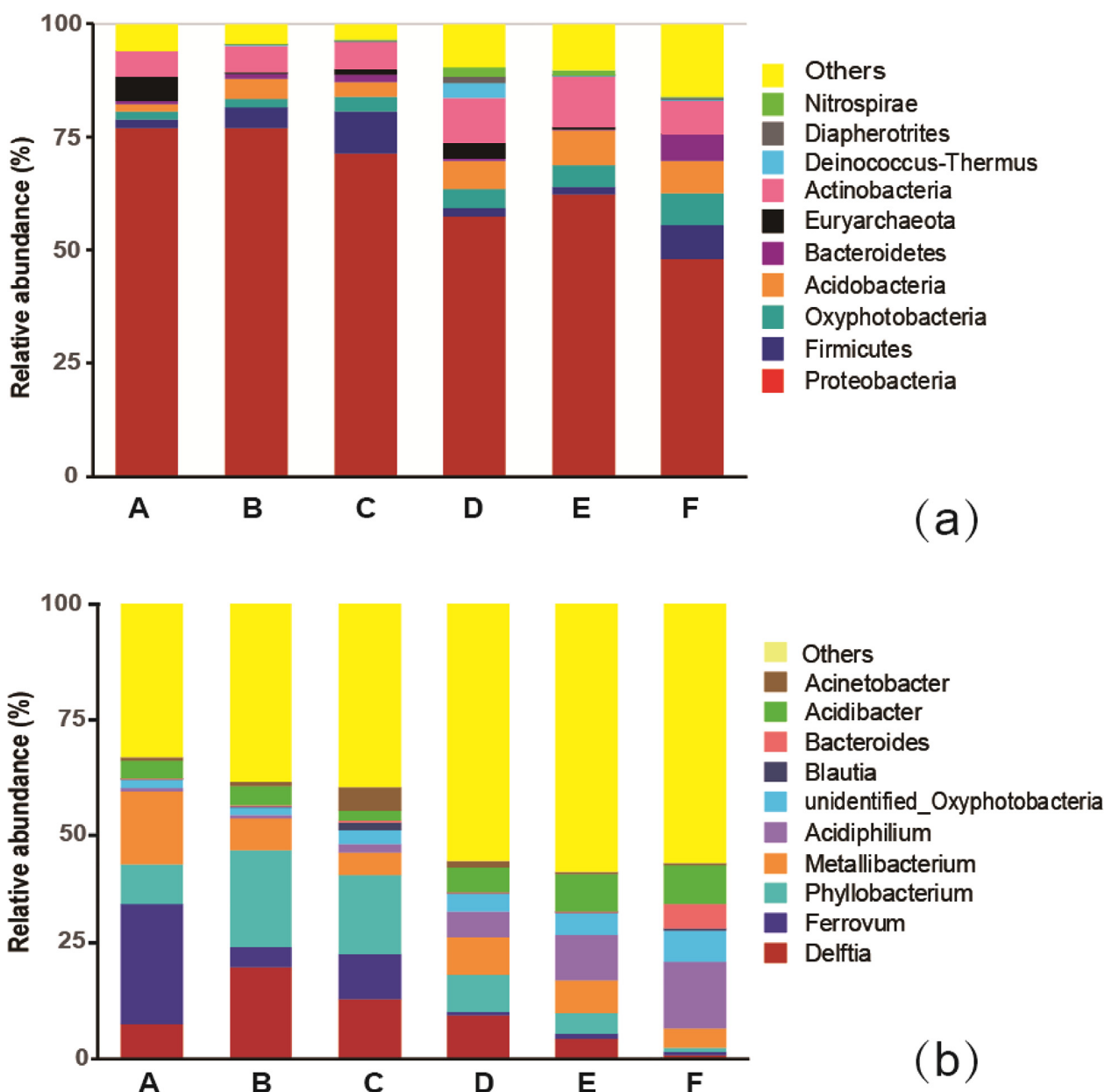
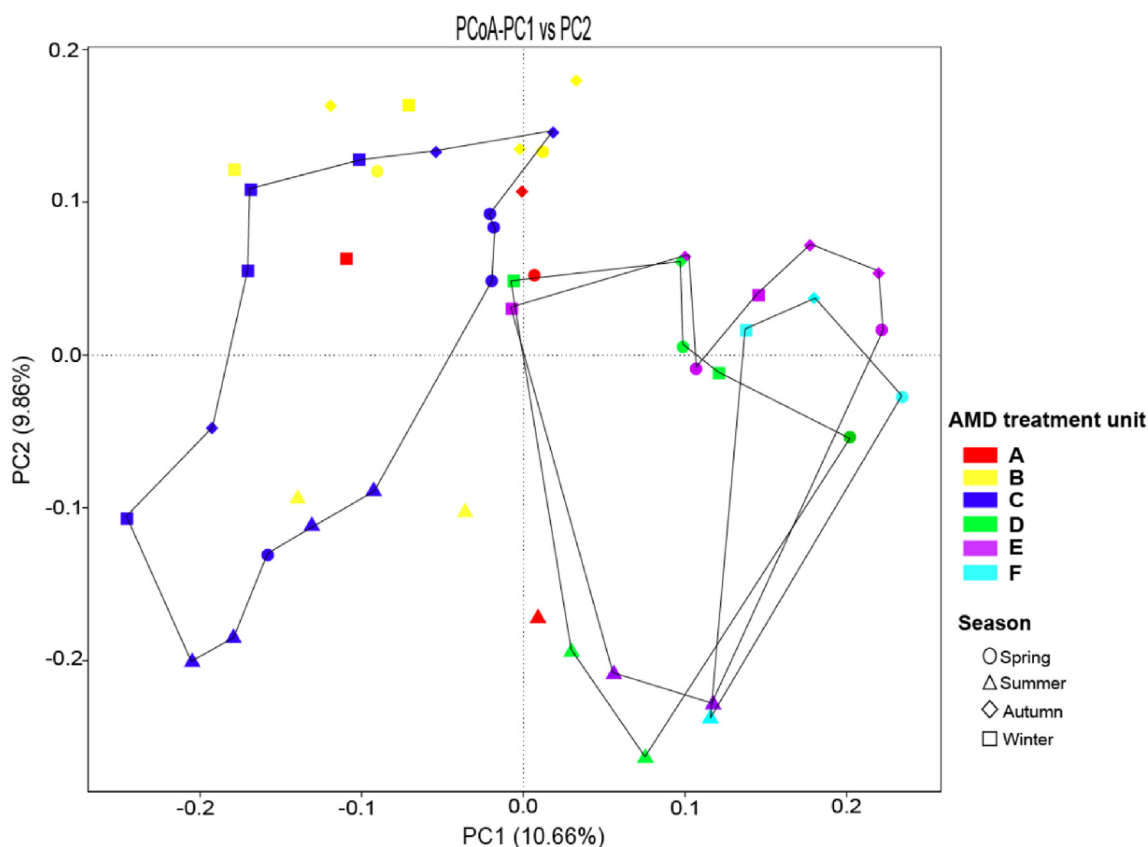


Fig. 3. MRA (%) of dominant lineages in different AMD treatment units of treatment system. (a): Phylum level; (b): genus level (A. coal adit; B. slope; C. pre-oxidation precipitation units; D. oxidation-precipitation units; E. ARUM units; F. setting unit).

within this treatment system in different seasons (Fig. 5a). During winter and spring, the microbial community was dominated by *Phyllobacterium* and *Delftia* (Fig. 5b). In summer the two genera declined (both MRA% < 5%), and the dominated genera shifted to *Metallibacterium* ( $11.73 \pm 8.12\%$ ), *Ferrofum* ( $9.98 \pm 12.23\%$ ) and *Acidibacter* ( $6.19 \pm 4.7\%$ ). In autumn, *Phyllobacterium* ( $9.14 \pm 12\%$ ) replaced *Acidibacter* ( $4.45 \pm 2.98\%$ ), and together with *Ferrofum* ( $10.54 \pm 14.94\%$ ) and *Metallibacterium* ( $8.47 \pm 6.03\%$ ), they became the top three genera. *Acidiphilium* was shown during the whole year and it flourished in spring with an MRA of  $6.51 \pm 8.47\%$ .

The results (Figs. 3-4) showed that the microbial consortia in the coal adit were distinct from that in the system. Even within the system in different units, the microbial compositions showed differences. The microbial consortia also differed in different seasons (Fig. 5). Analysing the possible metabolic preference of the microbial communities can help to better understand the differences in microbial consortia and figure out functions of the microbial consortia in the system. Since the detected microorganisms were not isolated and cultured, hints of their

potential metabolic preference could only be found from their reported relatives. It was mentioned before that Fe(II) oxidation and Fe removal were mainly achieved in the first two units. Moreover, Fe(II) oxidation was almost entirely achieved in the pre-oxidation precipitation units (cascades #1-4). Accordingly, Fe(II) oxidizer containing genera such as *Ferrofum*, *Acinetobacter* and *Metallibacterium* were found to be dominant in this unit. Research shows that *Ferrofum* species often appear in environments with high Fe(II) concentrations (> 230 mg/L); these species can only grow in the presence of Fe(II), and their iron oxidation rate is high (Johnson et al., 2014; Jones et al., 2015; Sheng et al., 2016). *Ferrofum* was frequently found to be enriched in AMD treatment bioreactors (Sun et al., 2016a; Sheng et al., 2016; Grettenberger et al., 2017), which indicates the importance of *Ferrofum* species in AMD treatment with engineered systems. Bacteria from *Acinetobacter* are tolerant of heavy metals at low pH and can promote Fe oxidation under anaerobic conditions (Su et al., 2015). However, in the pre-oxidation precipitation units, *Acinetobacter* was much less abundant than *Ferrofum*. Members from the genus *Metallibacterium* show versatile



**Fig. 4.** PCoA plot showing clusters of microbial communities based on unweighted UniFrac with 100% support at all nodes (A. coal adit; B. the slope; C. pre-oxidation precipitation units; D. oxidation-precipitation units; E. ARUM units; F. setting unit).

metabolisms. These species not only grow by utilizing organic compounds but also by oxidizing Fe(II) and reduced inorganic sulfur compounds (RISCs) and reducing Fe(III) (Ziegler et al., 2013; Brantner and Senko, 2014; Bartsch et al., 2017). Thus, the abovementioned Fe(II) oxidizer increased the removal of Fe(II) in the entire treatment system by accelerating the oxidation of Fe(II) to Fe(III) in this unit. In addition, the Fe(II) removal effect of the entire treatment system was better in summer and autumn (Fig. 2b), which may be related to *Ferrovum* and *Metallibacterium* being dominant in these two seasons (Fig. 5). Sulfur oxidation might also occur in this unit, which was indicated by the detection of the sulfur-oxidizer-containing genus *Delftia*. Microorganisms of *Delftia* are not generally known as sulfur oxidizers. However, a newly reported facultative chemolithoautotrophic mesophile *Delftia* sp. strain SR4, isolated from coal mine spoil, can use thiosulfate, elemental sulfur and tetrathionate as energy sources (Roy and Roy, 2019). The habitat of *Delftia* species in this study is very similar to that of the reported strain. The decreased pH and increased amount of  $\text{SO}_4^{2-}$  in sediments also indicated occurrences of sulfur oxidation.

In the oxidation-precipitation units (OC #1–2), the microbial consortia were still dominated by sulfur and iron oxidizers since the genera *Delftia* and *Metallibacterium* showed relatively high abundance. Fe(III) reduction have occurred since the genera of *Acidiphilium* and *Acidibacter* were detected. *Acidiphilium* generally exists in AMD and other acidic environments (Johnson, 1998; Johnson and Hallberg, 2003), and several species have been isolated (Okamura et al., 2015). Microorganisms from this genus can reduce iron and promote its dissolution in acidic environments (González et al., 2015). Bacteria of *Acidibacter* are categorized as acidophilic, mesophilic and obligately heterotrophic and can reduce Fe(III). It was reported that *Acidibacter ferrireducens* sp. Nov., isolated from mine environments, can catalyze the reductive dissolution of schwertmannite under microaerobic and anaerobic conditions (Falagan and Johnson, 2014). Although the microbial metabolism of

iron in the oxidation-precipitation units was still dominated by Fe(II) oxidation, the reduction of Fe(III) caused by *Acidiphilium* and *Acidibacter* may slow the further removal of Fe in this unit. This was in accordance with the practical environmental monitoring results showing that the removal efficiency of iron in the oxidation-precipitation stage is lower than that in the pre-oxidation precipitation stage (Fig. 2a).

In the ARUM units (MC #1–2), rice straw compost and the floating cattail mat caused the water to contain a high content of organic carbon and a low content of oxygen, which was quite different from the water in the first two units. A declining Eh also indicated a less oxidized environment in this unit than in the previous unit. Accordingly, a robust growth of facultative chemolithoautotrophic and anaerobic bacteria from the genera *Acidiphilium*, *Acidibacter* and *Metallibacterium* were detected. Alkalinity was generated while the Fe(III) was reduced (Akcil and Koldas, 2006), which was in accordance with the decrease in pH (Fig. 2c). With alkalinity generation, sulfides precipitated Fe(II) as iron sulfides. Consequently, concentrations of both sulfate and Fe in the AMD could be reduced in this unit. Notably, *Acidiphilium* in this treatment system flourished and dominated in the spring, which may have promoted the reduction of Fe(III) and inhibited the precipitation process of Fe(III), resulting in the worst performance of Fe removal of the treatment system in this season (Fig. 2a). The amount of  $\text{SO}_4^{2-}$  in sediment from this unit also decreased.

In the last unit (setting cell), *Acidiphilium*, *Acidibacter* and *Metallibacterium* were still the dominant genera but the growth of *Acidiphilium* increased and the growth of *Metallibacterium* decreased. Therefore, the AMD treatment of this unit strengthened the ARUM process and further increased the pH value of water. Notably, the distinct genus *Bacteroides* developed in this unit, which is related to the addition of rice straw. Bacteria of *Bacteroides* are often isolated from rice-straw residue and can utilize a wide variety of compounds as

**Table 2**  
MRA (%) of the dominant genus in the different AMD treatment units of the pilot-scale passive system.

Taxonomy	<i>Delftia</i>	<i>Ferroplasma</i>	<i>Phyllobacterium</i>	<i>Metallibacterium</i>	<i>Acidiphilium</i>	unidentified_Oxyphotobacteria	<i>Blautia</i>	<i>Bacteroides</i>	<i>Acidibacter</i>	<i>Acinetobacter</i>	Others
A	7.57 ± 10.5	26.59 ± 15.66	8.52 ± 12.49	16.13 ± 10.34	0.78 ± 0.44	1.76 ± 0.62	00.09 ± 0.09	0.13 ± 0.13	4.16 ± 1.62	0.59 ± 0.6	33.68 ± 6.98
B	20.18 ± 15.74	4.48 ± 6.44	21.26 ± 15.51	7.05 ± 7.98	0.63 ± 0.47	1.71 ± 4.02	00.23 ± 00.28	0.17 ± 0.18	4.19 ± 6.15	1.03 ± 0.98	39.07 ± 16.33
C	13.03 ± 10.6	9.83 ± 11.23	17.59 ± 12.00	4.91 ± 4.52	1.79 ± 2.68	3.17 ± 6.51	1.67 ± 5.22	0.52 ± 0.86	2.05 ± 1.11	5.2 ± 5.48	40.25 ± 11.76
D	9.53 ± 10.09	0.67 ± 0.42	8.29 ± 9.03	8.23 ± 7.02	5.62 ± 4.82	4.07 ± 4.24	0.1 ± 0.12	0.1 ± 0.09	5.35 ± 2.94	1.52 ± 2.14	56.53 ± 14.97
E	4.28 ± 8.09	1.2 ± 0.49	4.52 ± 8.3	7.33 ± 4.68	9.88 ± 6.95	4.86 ± 5.93	0.11 ± 0.15	0.1 ± 0.17	8.43 ± 4.19	0.44 ± 0.35	58.84 ± 10.08
F	0.8 ± 0.54	0.71 ± 0.24	0.86 ± 0.58	4.22 ± 1.02	14.66 ± 08.57	6.87 ± 5.8	0.52 ± 0.78	5.48 ± 9.56	8.48 ± 3.79	0.32 ± 0.29	57.06 ± 10.83

A. coal adit; B. slope; C. pre-oxidation precipitation units; D. oxidation precipitation units; E. ARUM units; F. setting unit.

carbon and energy sources including crystalline cellulose and lignocellulosic materials in the form of corncobs, corn hulls and rice straw (Ueki et al., 2008; Ueki et al., 2011). Their appearance indicated that successful fermentation occurred in the third unit.

Surprisingly, *Phyllobacterium* was the most abundant genus in the pre-oxidation precipitation units, and it also showed relatively high abundance in the oxidation-precipitation and ARUM units. Members of *Phyllobacterium* are well known as plant growth-promoting rhizobacteria (PGPR) for their N fixing capability (Mantelin et al., 2006). They were also detected in AMD-contaminated areas (Zhang et al., 2018; Hou et al., 2019). However, there is no detailed information on their remediation performance. Only one paper suggested that *Phyllobacterium myrsinacearum* RC6b is a good candidate for microbially assisted phytoremediation, because it enhanced growth and the Cd and Zn uptake of *Sedum plumbizincicola* (Ma et al., 2013). In this study, the genus *Phyllobacterium* was originally detected in the coal adit, which is covered by trees. Its growth enhanced at the slope terrain where various wild plants are growing aside the AMD stream, but its relative abundance kept decreasing along the system. Plants were observed growing at the inner edge of the first unit. Except for the growth of plants, in our study, no additional data supported the observation that the microorganisms could enhance the growth of plants. The role of this genus during the AMD treatment in the treatment system is not known, and its impact on the performance of the system will not be discussed at this time. It seems that *Phyllobacterium* were carried by the AMD stream from the slope terrain.

### 3.3. Effects of geochemical parameters on microbial community compositions

The results of classical canonical correlation analysis (CCA) in Fig. 6 demonstrated the possible correlations between geochemical parameters and bacterial community structure. Axis 1 explained 36% of the genus-level variability and was positively correlated with pH, TC, T, TN and  $SO_4^{2-}$  but negatively correlated with Eh, TH, TS and the rest of Fe-extractable fractions. Axis 2 explained a further 25.33% of the variability and was negatively correlated with all tested parameters except pH. As indicated by the length of the environmental variables' arrows in the CCA biplot, the stronger determinants for the microbial communities were  $Fe_{tot}$ , TS, FeOX1, T and FeOX2. The dominant genera of *Phyllobacterium* and *Delftia* were negatively correlated with pH ( $p < 0.01$ ) and temperature ( $p < 0.01$ ), and positively correlated with  $Fe_{tot}$ , FeOX1 and TS ( $p < 0.01$ ). *Acinetobacter* was positively correlated with TS,  $Fe_{tot}$ ,  $Fe_{card+AVS}$ , FeOX1 and  $Fe_{mag}$  ( $p < 0.01$ ), while negatively correlated with pH and temperature ( $p < 0.01$ ). *Metallibacterium* was significantly and positively correlated with temperature ( $p < 0.01$ ). Genera of *Ferroplasma* were positively correlated with  $Fe_{tot}$ , FeOX1 and FeOX2 ( $p < 0.01$ ). The microbes were mainly enriched in the (pre)oxidation precipitation units. In addition, *Acidibacter*, mainly distributed in the ARUM units and the setting unit, were positively correlated with pH ( $p < 0.05$ ) and negatively correlated with  $Fe_{tot}$  ( $p < 0.01$ ), FeOX1 ( $p < 0.01$ ),  $Fe_{card+AVS}$  ( $p < 0.01$ ), FeOX1 ( $p < 0.05$ ) and TS ( $p < 0.01$ ).

CCA exhibited that pH drove the change of microbial community composition in the pilot system (Fig. 6), in accord with findings that pH is usually a dominant parameter that affects the microbial community composition and diversity in AMD-contaminated areas as well as AMD treatment bioreactors (Sun et al., 2016a; Grottenberger et al., 2017). However, it is worth noting that variation in pH within the system was no more than one unit, so pH was not a unique determinative variable in shaping the microbial consortia within the system. Notably, microbial consortia were significantly linked to FeOX1 and FeOX2, which is consistent with previous findings that metal speciation affects microbial diversity and composition (Bier et al., 2015; Sun et al., 2016b). Microbial communities from the (pre)oxidation precipitation units were positively correlated with iron, and the elevated Fe contents in these



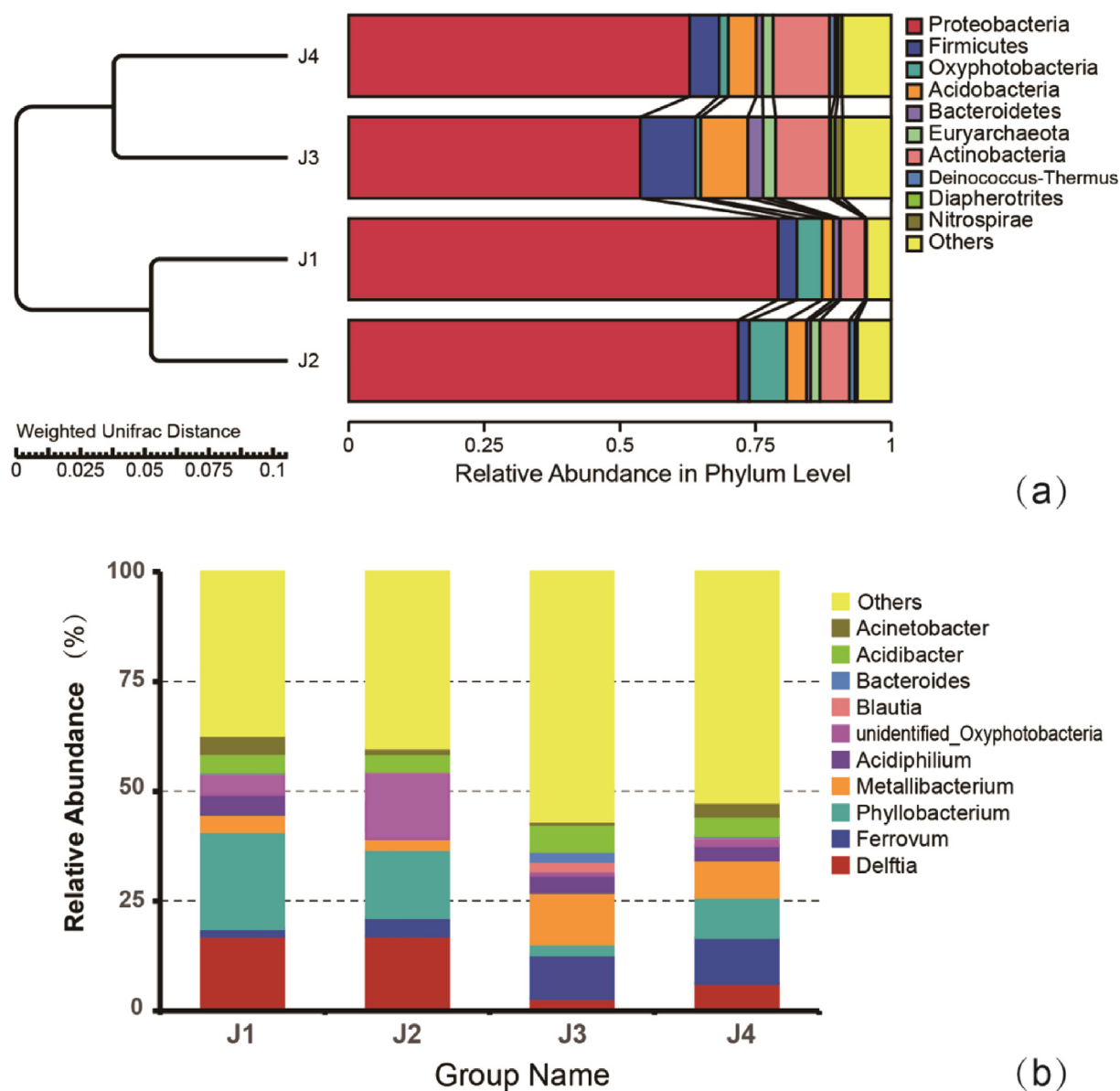


Fig. 5. (a) The UPGMA tree showing clusters of microbial communities based on weighted UniFrac from different seasons; (b) bacterial community composition of treatment system in different seasons based on relative abundance of bacterial class with top 10 genus (J1: Winter; J2: Spring; J3: Summer; J4: Autumn).

units favored the growth of various Fe-oxidizing bacteria (FeOB). For instance, *Ferroplasma* dominated in the cascades #1–4 and the oxidation-precipitation units, whereas the relative abundance in ARUM and the setting unit were relatively low. Moreover, the total S content was also found to be an influential factor in shaping microbial communities in the system. This is understandable because RISCs are energy sources and electron donors for sulfur oxidizing acidophiles and sulfate is an important electron receptor for SRB. Microbial sulfur metabolism is critical for the treatment of AMD (Sanchez-Andrea et al., 2014; Zhou et al., 2018). Similarly Fe(II), as the sole energy source and electron donor for chemolithotrophs, was also found to be a factor affecting the distribution of the microbial communities. During the monitoring period it was observed that microbial composition was influenced by seasonal succession. In fact, seasonal succession dramatically affected the temperature (Fig. 2f), which was responsible for seasonally ecological succession (Volant et al., 2014). For instance, the optimized growth temperature for *Ferroplasma* and *Metallibacterium* is in a range of 25–30 °C (Ziegler et al., 2013; Johnson et al., 2014). Accordingly, in the treatment system, the two genera were abundant in summer and

autumn when the temperature was approximately 25 °C. In addition, seasonal succession also affected the hydraulic retention time (HRT), which is related to the flow rate of the effluent in the system, and HRT affects the stability of passive bioreactors and their microbial communities (Vasquez et al., 2018). Thus, multiple physicochemical parameters jointly drove the variation of microbial consortia in this system.

#### 3.4. Several strategies to enhance the performance of the treatment system

From this study, the *in-situ* pilot-scale passive treatment system showed poor performance in the removal of sulfate as well as neutralization of acid. As we mentioned previously, the goals were expected to be achieved in the ARUM units (MC #1–2) by alkalinity-generating bacteria such as SRB and FeRB. Microbial community analysis showed that SRBs, the key microorganisms for sulfate removal, did not develop in this unit. The absence of SRB illustrates that the decreased sulfate in the effluent was probably precipitated via physicochemical interactions such as absorption by iron hydroxide particles and chelation by organic compounds. The monitored physicochemical

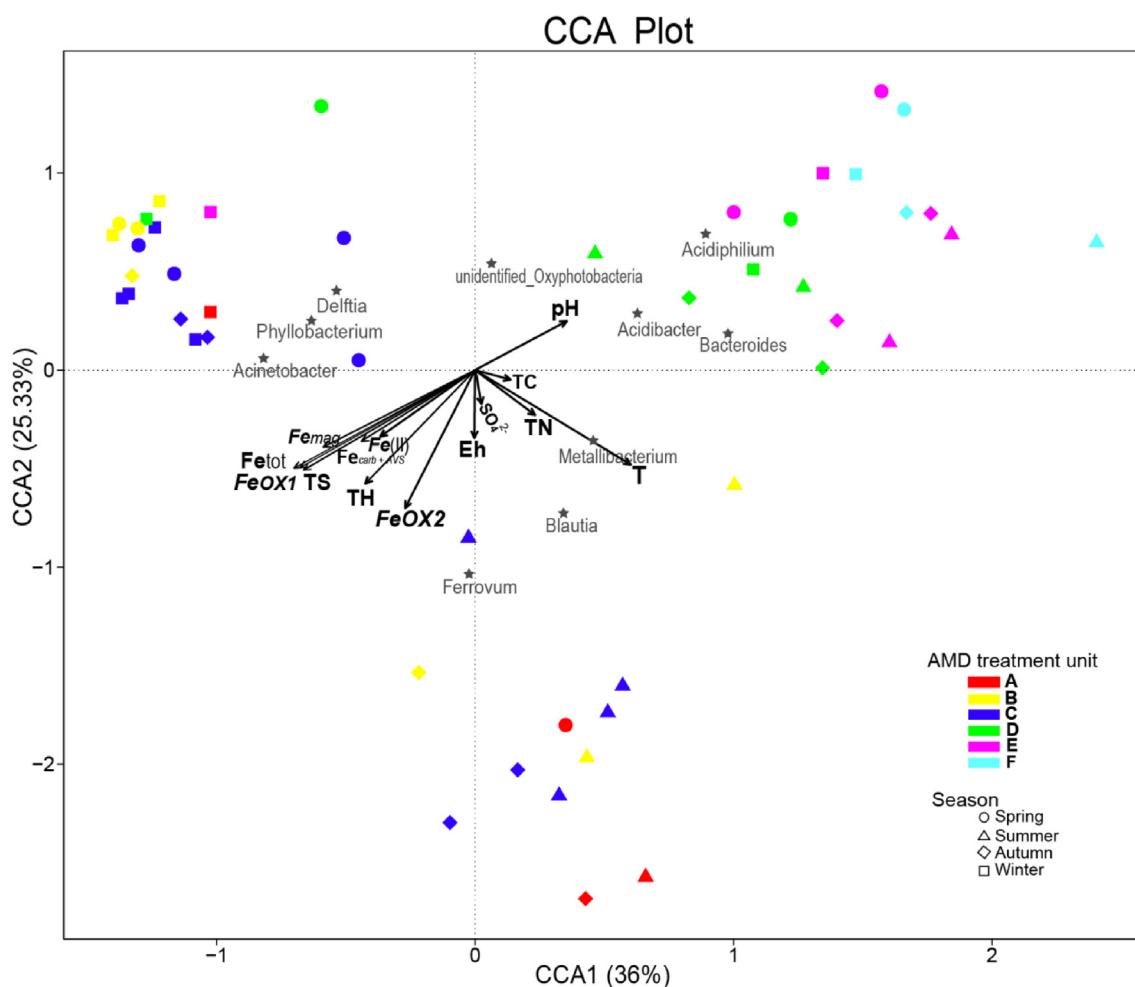


**Fig. 6.** Diagrams from CCA of relative abundances of dominant at genus level and major physicochemical parameters. Arrows designate direction and magnitude of geochemical parameters connected with bacterial community structures. Each sample is color-coded according to sampling area. (A. coal adit; B. slope; C. pre-oxidation precipitation units; D. oxidation-precipitation units; E. ARUM units; F. setting unit).

parameters indicated that low pH should be a crucial cause for the failure of the growth of SRB. The optimal growth pH for SRB is from 5.0 to 9.0 (Grossman and Postgate, 1953). Thus, increasing the pH to ensure the growth of SRB should be examined in the future. The introduction of limestone into the system could be a good strategy. The importance of limestone gravel berms was also emphasized when an ARUM treatment system was successfully applied to treat AMD (Kalin and Caetano Chaves, 2003). In this study, most of the Fe was oxidized in the pre-oxidation precipitation units. Some changes could probably be made in the oxidation-precipitation units to endow them with two functions: 1) precipitate Fe and 2) neutralize acidity. To achieve this goal, more curtains could be added to OC #1 to improve Fe removal. Moreover, OC #2 could be converted to a microbial cell with the addition of limestone gravel beneath the organic substrate or mixed with the organic substrate. In addition, SRB cannot degrade biopolymers directly, and their growth relies on the activity of anaerobic hydrolytic and fermentative bacteria such as *Clostridia* (Labrenz and Banfield, 2004). A mixture of organic substrate could be used since the presence of organic matter determines the growth of the anaerobic microflora, and higher sulfate reduction has been detected if the reactive mixtures contained more than one organic carbon source (Muhammad et al., 2015).

#### 4. Conclusions

Distinct microbial communities were shaped within a field pilot-

scale passive system and showed great influence on the performance of AMD *in-situ* bioremediation. Development of iron oxidizer enabled stable and effective cleanup of total soluble iron and Fe(II), while the absence of SRB caused a failure of sulfate removal and acidity neutralization. Multiple parameters including pH, iron speciation, TS and season succession jointly affected the microbial community structure. Moreover, several strategies were discussed to fix the growth problem of SRB. These results will promote the further development and application of *in-situ* field bioreactors to remediate AMD.

#### CRedit authorship contribution statement

**Haiyan Chen:** Conceptualization, Methodology, Software, Data curation, Writing - original draft. **Tangfu Xiao:** Writing - review & editing, Supervision, Funding acquisition. **Zengping Ning:** Methodology, Writing - review & editing. **Qian Li:** Formal analysis, Writing - review & editing. **Enzong Xiao:** Methodology, Formal analysis. **Yizhang Liu:** Data curation, Validation. **Qingxiang Xiao:** Formal analysis, Software, Validation. **Xiaolong Lan:** Data curation, Investigation. **Liang Ma:** Data curation, Investigation. **Fanghai Lu:** Data curation, Investigation.

#### Declaration of Competing Interest

The authors declare that they have no known competing financial interests or personal relationships that could have appeared to

influence the work reported in this paper.

## Acknowledgments

This work was supported by the National Natural Science Foundation of China (41830753, U1612442). The authors would like to thank Prof. Margarete Kalin, Dr. Bill Wheeler, and Dr. Carlos Paulo at the Boojum Research Ltd., and Prof. Wolfgang Sand at Biofilm Centre, Aquatische Biotechnologie, Universität Duisburg-Essen, Germany for technical support.

## Appendix A. Supplementary data

Supplementary data to this article can be found online at <https://doi.org/10.1016/j.biortech.2020.123985>.

## References

- Akcil, A., Koldas, S., 2006. Acid Mine Drainage (AMD): causes, treatment and case studies. *J. Clean. Prod.* 14, 1139–1145.
- Bai, H., Kang, Y., Quan, H., Han, Y., Sun, J., Feng, Y., 2013. Treatment of acid mine drainage by sulfate reducing bacteria with iron in bench scale runs. *Bioresour. Technol.* 128, 818–822.
- Bartsch, S., Gensch, A., Stephan, S., Doetsch, A., Gescher, J., 2017. *Metallibacterium scheffleri*: genomic data reveal a versatile metabolism. *FEMS Microbiol. Ecol.* 93, fix011.
- Behum, P.T., Lefticariu, L., Bender, K.S., Segid, Y.T., Burns, A.S., Pugh, C.W., 2011. Remediation of coal-mine drainage by a sulfate-reducing bioreactor: A case study from the Illinois coal basin, USA. *Appl. Geochem.* 26, S162–S166.
- Bier, R.L., Voss, K.A., Bernhardt, E.S., 2015. Bacterial community responses to a gradient of alkaline mountaintop mine drainage in Central Appalachian streams. *ISME J.* 9, 1378–1390.
- Brantner, J.S., Senko, J.M., 2014. Response of soil-associated microbial communities to intrusion of coal mine-derived acid mine drainage. *Environ. Sci. Tech.* 48, 8556–8563.
- Caporaso, J.G., Kuczynski, J., Stombaugh, J., Bittinger, K., Bushman, F.D., Costello, E.K., Fierer, N., Pena, A.G., Goodrich, J.K., Gordon, J.I., Huttley, G.A., Kelley, S.T., Knights, D., Koenig, J.E., Ley, R.E., Lozupone, C.A., McDonald, D., Muegge, B.D., Pirrung, M., Reeder, J., Sevinsky, J.R., Turnbaugh, P.J., Walters, W.A., Widmann, J., Yatsunenko, T., Zaneveld, J., Knight, R., 2010. QIIME allows analysis of high-throughput community sequencing data. *Nat. Methods* 7, 335–336.
- Caporaso, J.G., Lauber, C.L., Walters, W.A., Berg-Lyons, D., Huntley, J., Fierer, N., Owens, S.M., Betley, J., Fraser, L., Bauer, M., Gormley, N., Gilbert, J.A., Smith, G., Knight, R., 2012. Ultra-high-throughput microbial community analysis on the Illumina HiSeq and MiSeq platforms. *ISME J.* 6, 1621–1624.
- Edgar, R.C., 2013. UPARSE: highly accurate OTU sequences from microbial amplicon reads. *Nat. Methods* 10, 996–998.
- Edgar, R.C., Haas, B.J., Clemente, J.C., Quince, C., Knight, R., 2011. UCHIME improves sensitivity and speed of chimera detection. *Bioinformatics* 27, 2194–2200.
- Falagan, C., Johnson, D.B., 2014. *Acidibacter ferrireducens* gen. nov., sp. nov.: an acidophilic ferric iron-reducing gammaproteobacterium. *Extremophiles* 18, 1067–1073.
- Favas, P.J.C., Sarkar, S.K., Rakshit, D., Venkatchalam, P., Prasad, M.N.V., 2016. Acid Mine Drainages From Abandoned Mines. *Environ. Mater. Waste.* 413–462.
- Gazea, B., Adam, K., Kontopoulos, A., 1996. A review of passive systems for the treatment of acid mine drainage. *Miner. Eng.* 9, 23–42.
- González, E., Espada, A., Muñoz, J.Á., Blázquez, M.L., González, F., Ballester, A., 2015. Reductive dissolution of magnetite and jarosite by *Acidiphilium cryptum* JF-5. *Hydrometallurgy* 157, 292–297.
- Grettenberger, C., Pearce, A., Bibby, K., Jones, D., Burgos, W., Macalady, J., 2017. Efficient Low-pH Iron Removal by a Microbial Iron Oxide Mound Ecosystem at Scalp Level Run. *Appl. Environ. Microbiol.* 83, e00015–e17.
- Grossman, J.P., Postgate, J.R., 1953. The estimation of sulphate-reducing bacteria (*D. desulphuricans*). *J. Appl. Bacter.* 16, 1–9.
- Haas, B.J., Gevers, D., Earl, A.M., Feldgarden, M., Ward, D.V., Giannoukos, G., Ciulla, D., Tabbaa, D., Highlander, S.K., Sodergren, E., Methe, B., DeSantis, T.Z., Human Microbiome, C., Petrosino, J.F., Knight, R., Birren, B.W., 2011. Chimeric 16S rRNA sequence formation and detection in Sanger and 454-pyrosequenced PCR amplicons. *Genome Res.* 21, 494–504.
- Hou, D., Zhang, P., Zhang, J., Zhou, Y., Yang, Y., Mao, Q., Tsang, D.C.W., Nunez-Delgado, A., Luo, L., 2019. Spatial variation of sediment bacterial community in an acid mine drainage contaminated area and surrounding river basin. *J. Environ. Manage.* 251, 109542.
- Johnson, D.B., 1998. Biodiversity and ecology of acidophilic microorganisms. *FEMS Microbiol. Ecol.* 27, 307–317. Johnson, D.B., Hallberg, K.B. 2003. The microbiology of acidic mine waters. *Res. Microbiol.* 154, 466–473.
- Johnson, D.B., Hallberg, K.B., 2003. The microbiology of acidic mine waters. *Res. Microbiol.* 154, 466–473.
- Johnson, D.B., Hallberg, K.B., 2005. Acid mine drainage remediation options: a review. *Sci. Total Environ.* 338, 3–14.
- Johnson, D.B., Hallberg, K.B., Hedrich, S., 2014. Uncovering a microbial enigma: isolation and characterization of the streamer-generating, iron-oxidizing, acidophilic bacterium “*Ferroplasma myxofaciens*”. *Appl. Environ. Microbiol.* 80, 672–680.
- Jones, D.S., Kohl, C., Grettenberger, C., Larson, L.N., Burgos, W.D., Macalady, J.L., 2015. Geochemical niches of iron-oxidizing acidophiles in acidic coal mine drainage. *Appl. Environ. Microbiol.* 81, 1242–1250.
- Kalin, M., Caetano Chaves, W.L., 2003. Acid reduction using microbiology: treating AMD effluent emerging from an abandoned mine portal. *Hydrometallurgy* 71, 217–225.
- Kalin, M., Fyson, A., Wheeler, W.N., 2006. The chemistry of conventional and alternative treatment systems for the neutralization of acid mine drainage. *Sci. Total Environ.* 366, 395–408.
- Labrenz, M., Banfield, J.F., 2004. Sulfate-reducing bacteria-dominated biofilms that precipitate ZnS in a subsurface circumneutral-pH mine drainage system. *Microb. Ecol.* 47, 205–217.
- Larson, L.N., Sánchez-España, J., Burgos, W., 2014. Rates of low-pH biological Fe(II) oxidation in the Appalachian Bituminous Coal Basin and the Iberian Pyrite Belt. *Appl. Geochem.* 47, 85–98.
- Ma, Y., Rajkumar, M., Luo, Y., Freitas, H., 2013. Phytoextraction of heavy metal polluted soils using *Sedum plumbizincicola* inoculated with metal mobilizing *Phyllobacterium myrsinacearum* RC6b. *Chemosphere* 93, 1386–1392.
- Magoc, T., Salzberg, S.L., 2011. FLASH: fast length adjustment of short reads to improve genome assemblies. *Bioinformatics* 27, 2957–2963.
- Mantelin, S., Desbrosses, G., Larcher, M., Tranbarger, T.J., Cleyet-Marel, J.C., Touraine, B., 2006. Nitrate-dependent control of root architecture and N nutrition are altered by a plant growth-promoting *Phyllobacterium* sp. *Planta* 223, 591–603.
- Muhammad, S.N., Kusin, F.M., Zahar, M.S.M., Halimoon, N., Yusuf, F.M., 2015. Passive Treatment of Acid Mine Drainage Using Mixed Substrates: Batch Experiments. *Procedia Environ. Sci.* 30, 157–161.
- Okamura, K., Kawai, A., Wakao, N., Yamada, T., Hiraishi, A., 2015. *Acidiphilium iwatense* sp. nov., isolated from an acid mine drainage treatment plant, and emendation of the genus *Acidiphilium*. *Int. J. Syst. Evol. Microbiol.* 65, 42–48.
- Oni, O., Miyatake, T., Kasten, S., Richter-Heitmann, T., Fischer, D., Wagenknecht, L., Kulkarni, A., Blumers, M., Shylin, S.I., Ksenofontov, V., Costa, B.F., Klingelhofer, G., Friedrich, M.W., 2015. Distinct microbial populations are tightly linked to the profile of dissolved iron in the methanic sediments of the Helgoland mud area, North Sea. *Front. Microbiol.* 6, 365.
- Poulton, S.W., Canfield, D.E., 2005. Development of a sequential extraction procedure for iron: implications for iron partitioning in continentally derived particulates. *Chem. Geol.* 214, 209–221.
- Pruvot, C., Douay, F., Hervé, F., Waterlot, C., 2006. Heavy Metals in Soil, Crops and Grass as a Source of Human Exposure in the Former Mining Areas (6 pp). *J. Soils Sediments* 6, 215–220.
- Roy, S., Roy, M., 2019. Characterization of plant growth promoting feature of a neutrotrophic, facultatively chemolithoautotrophic, sulphur oxidizing bacterium *Delftia* sp. strain SR4 isolated from coal mine spoil. *Int. J. Phytorem.* 21, 531–540.
- Sanchez-Andrea, I., Sanz, J.L., Bijmans, M.F., Stams, A.J., 2014. Sulfate reduction at low pH to remediate acid mine drainage. *J. Hazard. Mater.* 269, 98–109.
- Sheng, Y., Bibby, K., Grettenberger, C., Kaley, B., Macalady, J.L., Wang, G., Burgos, W.D., 2016. Geochemical and Temporal Influences on the Enrichment of Acidophilic Iron-Oxidizing Bacterial Communities. *Appl. Environ. Microbiol.* 82, 3611–3621.
- Simate, G.S., Ndlovu, S., 2014. Acid mine drainage: Challenges and opportunities. *J. Environ. Chem. Eng.* 2, 1785–1803.
- Su, J., Zheng, S.C., Huang, T., Ma, F., Shao, S.C., Yang, S.F., Zhang, L., 2015. Characterization of the anaerobic denitrification bacterium *Acinetobacter* sp. SZ28 and its application for groundwater treatment. *Bioresour. Technol.* 192, 654–659.
- Sun, W., Xiao, E., Kalin, M., Krumins, V., Dong, Y., Ning, Z., Liu, T., Sun, M., Zhao, Y., Wu, S., Mao, J., Xiao, T., 2016a. Remediation of antimony-rich mine waters: Assessment of antimony removal and shifts in the microbial community of an onsite field-scale bioreactor. *Environ. Pollut.* 215, 213–222.
- Sun, W., Xiao, E., Krumins, V., Dong, Y., Xiao, T., Ning, Z., Chen, H., Xiao, Q., 2016b. Characterization of the microbial community composition and the distribution of Fe-metabolizing bacteria in a creek contaminated by acid mine drainage. *Appl. Microbiol. Biotechnol.* 100, 8523–8535.
- Tamura, H., Goto, K., Yotsuyanagi, T., Nagayama, M., 1974. Spectrophotometric determination of iron (II) with 1,10-phenanthroline in the presence of large amounts of iron (III). *Talanta* 21, 314–318.
- Ueki, A., Abe, K., Kaku, N., Watanabe, K., Ueki, K., 2008. *Bacteroides propionicifaciens* sp. nov., isolated from rice-straw residue in a methanogenic reactor treating waste from cattle farms. *Int. J. Syst. Evol. Microbiol.* 58, 346–352.
- Ueki, A., Abe, K., Ohtaki, Y., Kaku, N., Watanabe, K., Ueki, K., 2011. *Bacteroides paurosaccharolyticus* sp. nov., isolated from a methanogenic reactor treating waste from cattle farms. *Int. J. Syst. Evol. Microbiol.* 61, 448–453.
- Vasquez, Y., Escobar, M.C., Saenz, J.S., Quiceno-Vallejo, M.F., Neculita, C.M., Arbeli, Z., Roldan, F., 2018. Effect of hydraulic retention time on microbial community in biochemical passive reactors during treatment of acid mine drainage. *Bioresour. Technol.* 247, 624–632.
- Volant, A., Bruneel, O., Desoeuvre, A., Hery, M., Casiot, C., Bru, N., Delpoux, S., Fahy, A., Javerliat, F., Bouchez, O., Duran, R., Bertin, P.N., Elbaz-Poulichet, F., Lauga, B., 2014. Diversity and spatiotemporal dynamics of bacterial communities: physico-chemical and other drivers along an acid mine drainage. *FEMS Microbiol. Ecol.* 90, 247–263.
- Zhang, M., Chen, B., Wang, N., Chen, J., Zou, L., Liu, X., Wang, Z., Wen, J., Liu, W., 2018. Effects of heap-bioleaching plant on microbial community of the nearby river. *Int. Biodeterior. Biodegrad.* 128, 36–40.
- Zhou, H., Sheng, Y., Zhao, X., Gross, M., Wen, Z., 2018. Treatment of acidic sulfate-containing wastewater using revolving algae biofilm reactors: Sulfur removal performance and microbial community characterization. *Bioresour. Technol.* 264, 24–34.
- Ziegler, S., Waidner, B., Itoh, T., Schumann, P., Spring, S., Gescher, J., 2013. *Metallibacterium scheffleri* gen. nov., sp. nov., an alkalizing gammaproteobacterium isolated from an acidic biofilm. *Int. J. Syst. Evol. Microbiol.* 63, 1499–1504.